Interferometric testing of photomask substrate flatness

Article *in* Proceedings of SPIE - The International Society for Optical Engineering · August 2001

DOI: 10.1117/12.436725

5 authors, including:

Chris Evans
University of North Carolina at Charlotte

Robert E. Parks
The University of Arizona

Tony L. Schmitz
University of North Carolina at Charlotte

Angela Davies
University of North Carolina at Charlotte

Interferometric testing of photomask substrate flatness

Christopher J. Evans
Robert E. Parks
Lianzhen Shao
Tony L. Schmitz
Angela D. Davies

Interferometric Testing of Photomask Substrate Flatness

Chris J. Evans*, Robert E. Parks#, Lian-Zhen. Shao@, Tony Schmitz*, and Angela Davies*

* National Institute of Standards and Technology, Manufacturing Metrology Division, Stop 8220, Gaithersburg, MD 20899-8220
# Optical Perspectives Group, Tucson, AZ
@ Tucson Optical Research Corporation, Tucson, AZ

ABSTRACT

Conventional interferometric testing of the flatness of photomask substrates[$] is rendered difficult by the long coherence length of the HeNe laser sources typically used in commercially available phase measuring interferometers appropriate for flatness testing. The Ritchey-Common configuration allows testing of flats in a spherical wavefront; this paper shows that, under appropriate conditions, high resolution surface flatness maps of photomask substrates may be obtained using instrumentation currently available in many optical shops.

Keywords : photomasks, interferometry, flatness, Ritchey-Common test

1. INTRODUCTION

The trend toward decreasing wavelengths used in advanced steppers results in decreased depth of focus, suggesting that the allowed contribution to the overall system aberrations arising from the photomask substrate should decrease proportionally. In the specific case of extreme ultraviolet lithography (EUVL), the photomask will be reflective and, hence, the flatness requirements are much tighter. Photomask substrates are frequently measured using commercially available Abramson[1] grazing incidence interferometers; quoted uncertainties in these measurements[2] exceed the flatness requirement in the current draft SEMI standard for EUVL mask substrates[3] and for the EUVL beta test stepper currently under construction[4].

State of the art interferometric flatness measurements are typically made with Fizeau interferometers (see for example Mantravadi)[5], most commonly utlizing a HeNe laser with an operating wavelength of 633 nm. The beam splitter for such interferometers is also the reference surface of the so-called transmission flat (Figure 1(a)), which is translated using piezoelectric drives to provide fringe modulation. Reflectivity of the reference surface and an uncoated glass flat are similar, providing good fringe contrast. Such interferometers are widely used throughout the optics fabrication industry. Two difficulties face their use for photomask flatness metrology. First, photomasks are thin parallel plates and the coherence length of laser sources causes interference between front and rear surface reflections (Fig 1(b) (in addition to the desired interference between the reference and front surface reflections), producing a set of fringes that are not modulated by shifting the reference surface (Figures 1(c)-(e)). These static fringes, variously described as Haidinger or Fabry-Perot fringes, produce apparent wavefront variations that are not directly attributable to height variation in the front surface. Secondly, the vast majority of instruments in optical shops have 100 mm or 150 mm circular apertures; photomasks are typically 152 mm square, requiring a circular aperture of approximately 215 mm.

As previously discussed[6],the problems posed by rear surface reflections can be mitigated by using a short coherence length source in various interferometric configurations[7,8], mathematically deconvolving the contributions of the two reflections based on precise positioning of the part under test[9], using grating interferometers[10], or using a diode source and an optical path difference (OPD) that is a multiple of the laser cavity length[11]. None of these approaches, however, can be implemented by users of He-Ne based instruments currently in service. Users of such instruments can frustrate the rear surface reflection using an appropriate index matching fluid or eliminate the reflection by coating the front surface with a highly reflective coating. However, both approaches require subsequent cleaning, and do not address the limited aperture of most instruments.

[$] Terminology is not consistent across the industry and the literature. In conformance with the SEMI standards group on EUVL masks, we use the term "substrate" for bare glass, saving "blank" to describe the multi-layer coated substrate and "mask" for the finished, patterned product

Here we present preliminary results showing that high resolution maps of photomask substrate flatness can be obtained using current HeNe based phase shifting interferometers in the Ritchey-Common configuration. The full area of a 152 mm square substrate can be measured using a 100 mm aperture interferometer and reflections from front and rear surfaces separated.

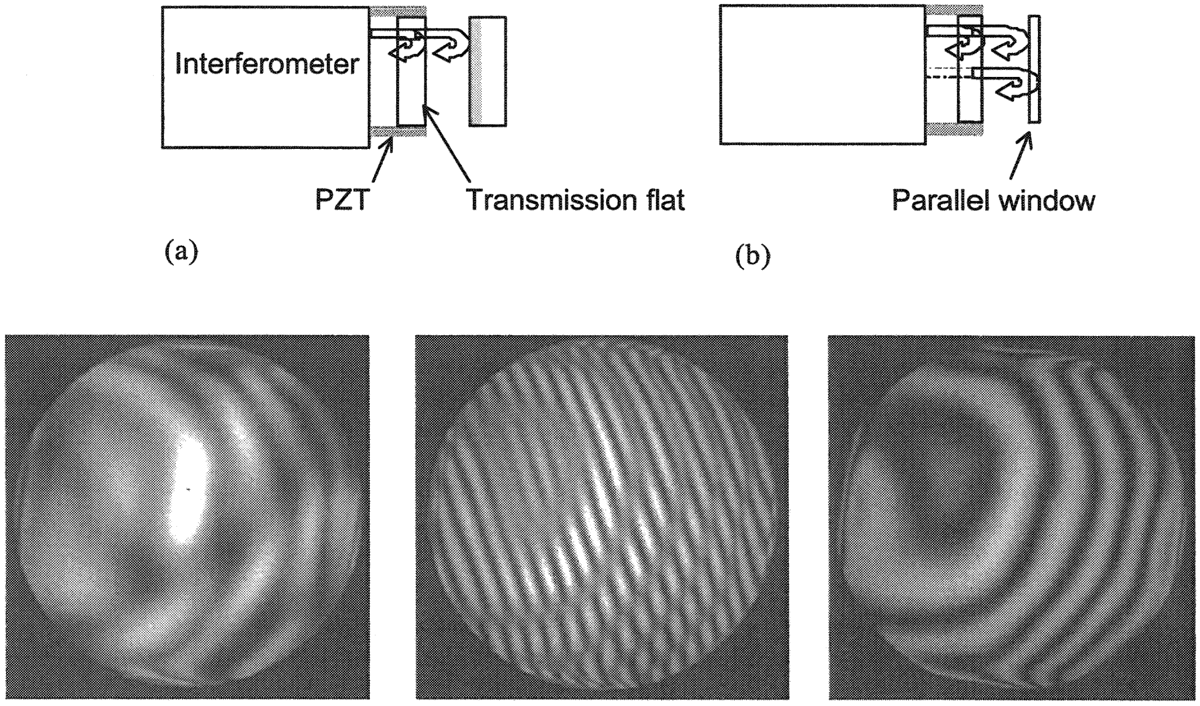

(c) (d) (e)

Figure 1 (a) Conventional Fizeau configuration and (b) additional reflection from rear surface of a thin parallel plate. (c) Observed fringe pattern with contributions from all three reflections. (d) Transmission flat tilted and (e) removed, showing interference between front and rear surfaces.

2. RITCHEY-COMMON TEST

The Ritchey-Common test[12] allows the interferometric measurement of a flat using a spherical wavefront. Its implementation on a modern, Fizeau phase measuring interferometer (PMI) is shown in Figure 2. A transmission sphere generates, beyond focus, a diverging beam into which the test flat is placed at an appropriate angle. The wavefront continues to diverge beyond the tilted flat until it reflects off a concave spherical surface and retraces its path into the interferometer imaging system (Measurement 2). The optical path difference introduced by flatness deviations h of the flat is $2h \cos a$, where a is a function of position on the part; this variation of sensitivity with position can easily be compensated in post-processing of phase data. In a separate measurement (Measurement 1), the return sphere is measured directly with the transmission sphere to allow separation of the surface departure of the flat from the errors of the interferometer, transmission sphere, and return sphere. The details of those calibration techniques will not be discussed here[13,14]. However, it has been demonstrated that a measurement of relatively low uncertainty[15] can be made of a flat of larger aperture than the selected commercially available PMI.

In addition to post-processing the data to compensate for varying sensitivity as a function of position, two other factors must be addressed: mapping the part to interferometer coordinates and isolating spherical (quadratic) shape contributions to flatness.

Coordinate mapping

For simplicity, consider first a circular flat, tilted as shown in Figure 2, that is the aperture stop in the system. Depending on its precise position with respect to the optical axis of the interferometer, it will appear as a distorted ellipse. A square flat

(Figure 3) will appear to be an irregular trapezoid with curved edges. This distortion can be more easily visualized by considering it as the projection of a tilted 152 mm square flat onto a spherical surface (Figure 3 (a)). Figure 3(b) shows the case where the photomask is centered; the smaller undistorted rectangle is the photomask in its own plane looking down the axis toward the source; the larger trapezoid is the projection on the sphere. Figure 3(c) shows the case where the substrate is displaced 25 mm above the axis.

Quadratic terms

Consider again a circular flat. At first sight it would appear that a quadratic term (ie power) in the test flat will be difficult to separate from imperfect spacing of the return sphere (which adds power to the interferogram). Because of the tilt, however, the quadratic term in the flat adds an astigmatic term in the wavefront which does not rotate as the part is rotated. The non-rotating component of astigmatism is used, therefore, to compute the power in the flat; the component that rotates is, of course, astigmatism in the part. For a square part, a similar pattern with two-fold symmetry will be observed.

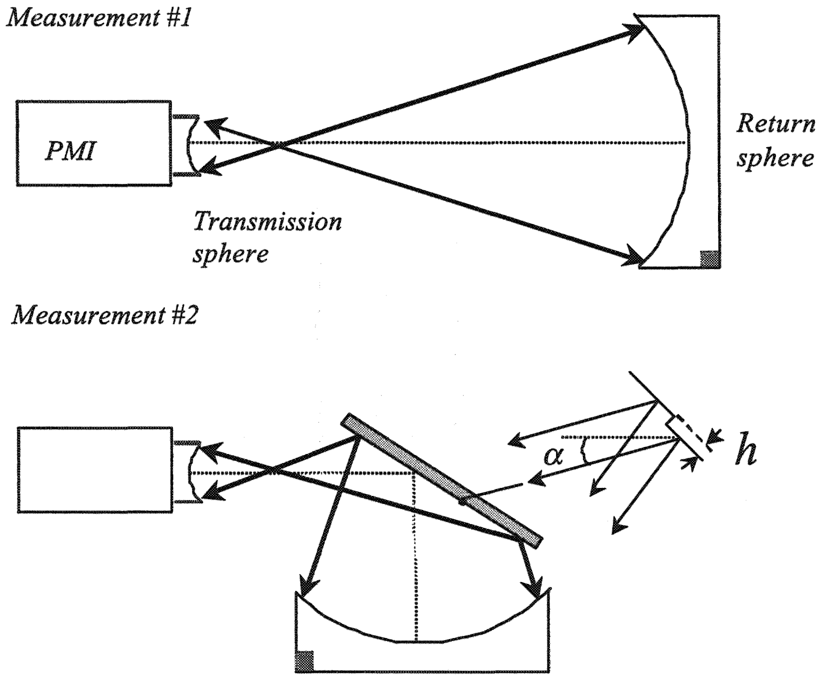

Figure 2 The two measurement positions of the Ritchey-Common test

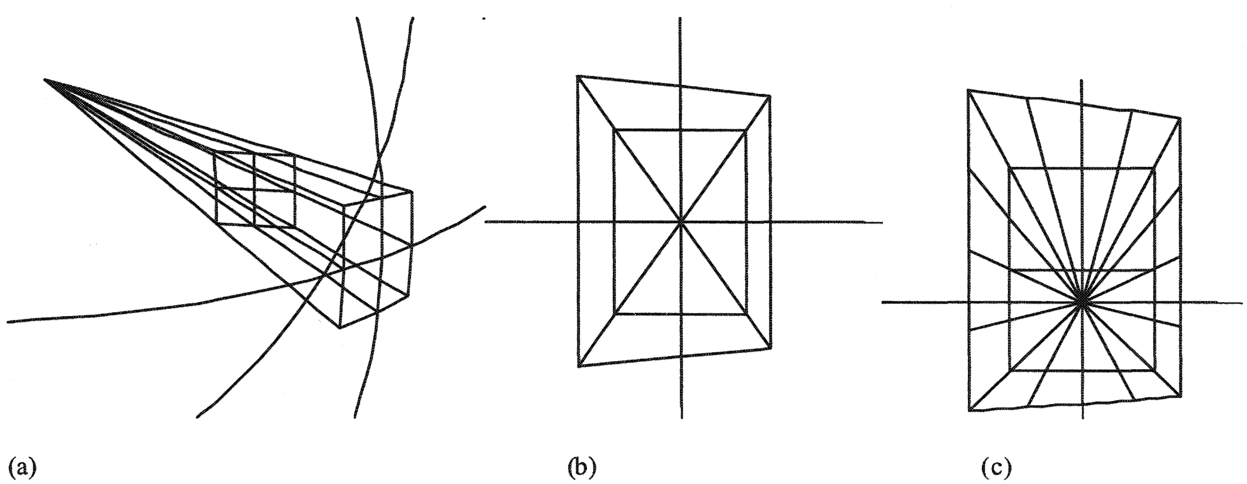

Figures 3 Coordinate mapping for a Ritchey-Common test of a square flat (a) viewed as a projection problem, (b) for a symmetrically located flat, and (c) with the flat displaced.

RITCHEY-COMMON TEST OF A TRANSPARENT FLAT

In the case of a transparent flat (photomask substrate), coherent reflections are possible from both front and rear surfaces of the flat. Figure 4 shows the hypothetical case (for a very small beam divergence and a glass of index 1) where the portion of the beam returning from the concave spherical mirror reflects off the rear surface of the plate and forms a focus that is displaced from the focus of the light from the front surface. The magnitude of this shift is determined by the thickness of the plate and the tilt angle; for the highly simplified case of Figure 4, this "stray" light can be prevented from returning into the interferometer using an appropriately placed beam block or "stop". Note, however, that this places a limit on the f-number of the transmission sphere that may be used since there are shifts both along and transverse to the original optical axis of the interferometer. In addition to the stray reflection shown in Figure 4, two other unwanted reflections can arise; rays reflecting off the rear surface on its way toward the return sphere and then the front surface (rear-front) and twice from the rear surface (rear-rear)

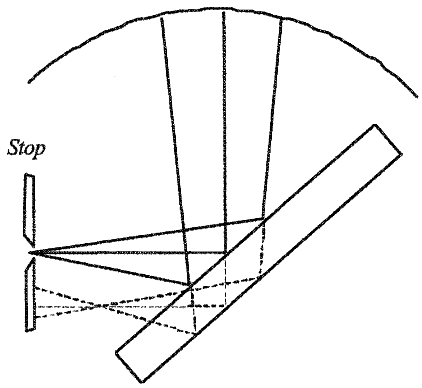

Figure 4 Formation of multiple foci

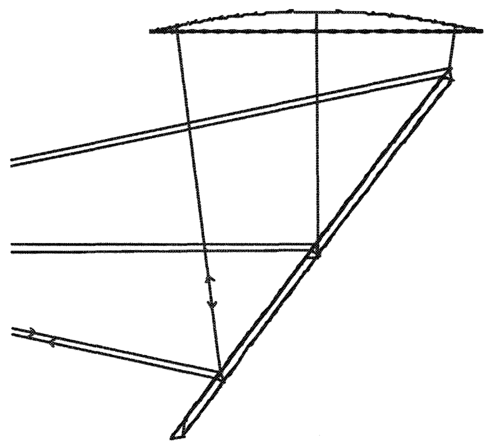

Figure 5 Rear surface reflections are abberated

For real glasses (n > 1), rays reflected off the rear surface will be refracted as they traverse the front surface (Figure 5), producing an aberrated wavefront with a focus displaced somewhat from the idealized position discussed above. The imperfect wavefront from the interferometer adds further aberrations. To test if these stray reflections can be eliminated by a beam blocking stop, a system using a 150 mm nominal aperture commercially available f/3.2 transmission sphere to measure 6.25 mm thick fused quartz mask substrates has been modeled using Zemax[16] optical design code. Figure 6 shows a close-up of the focii for the front-rear case showing a lateral separation of approximately 4.4 mm. For the f/3.2 cone, axial shift is clearly not a problem. A similar lateral separation is predicted for the rear-front reflections, and about twice that for rear-rear. The calculated image at the beam block (generated using the Zemax image analysis option) indicates that even for the rear-rear case, the aberrated spot (Figure 7) should not be so large as to be impossible to remove with a stop. Thus it appears that stray light will not be a problem for this measurement configuration.

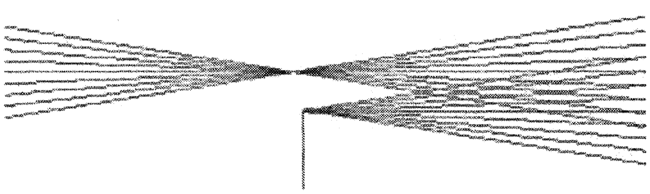

Figure 6: Separation of focii for front-rear reflections

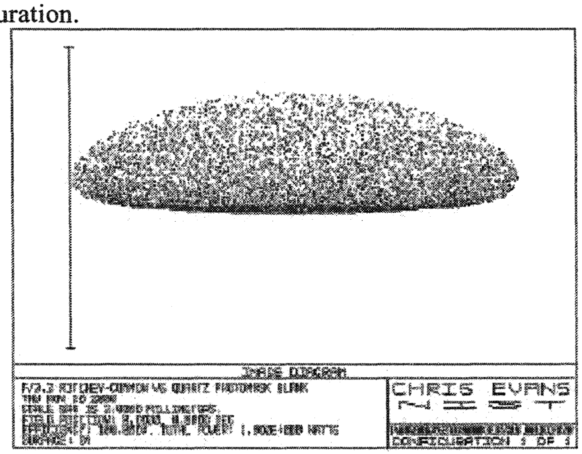

Figure 7 Rear-rear reflection image(scale bar is 2 mm)

A practical issue with the test configuration is reflectivity and fringe contrast. The photomask will have approximately 4% reflectivity at near normal incidence, as does the reference surface of the transmission sphere. A highly reflective (aluminized) return sphere must be used (assumed reflectivity of 95 %). The modulation, or fringe visibility, γ, is given by[17]:

$$\gamma = \frac{2A_r A_t}{(A_r^2 + A_t^2)}$$

where A_r and A_t are the wavefront amplitudes in the reference (i.e. from the transmission sphere) and test or return beams. Low contrast (ie low γ) typically results in a poor signal to noise ratio. Note that, for the assumed reflectivities indicated above, the calculated fringe visibility is very close to the default threshold for at least one commercially available PMI[18], 0.07.

For linearly polarized light, reflectivity is a function of both the incident angle and the plane of the polarization vector with respect to the plane of incidence. Figure 8 shows calculated fringe visibilities (dashed lines) as a function of the angle of incidence for two orthogonal polarizations and an assumed index n of 1.5. The test is double pass, so the increased reflectivity for TE transverse electric (TE) polarization (normal to the plane of incidence) gives a dramatic increase in fringe visibility as the angle increases above about 30 degrees. Increasing angle reduces amplitude (height) resolution (or scale factor), plotted as the upper solid line in Figure 8 relative to a conventional Fizeau cavity; also shown is the range over a flat that fills an f/3.3 cone of light. As angle increases, the effective pixel size increases (and lateral or spatial resolution decreases) in the tilt direction; this changing ratio of spatial resolutions (and its variation within an f/3.3 cone) is also plotted in Figure 8 as the lower solid line.

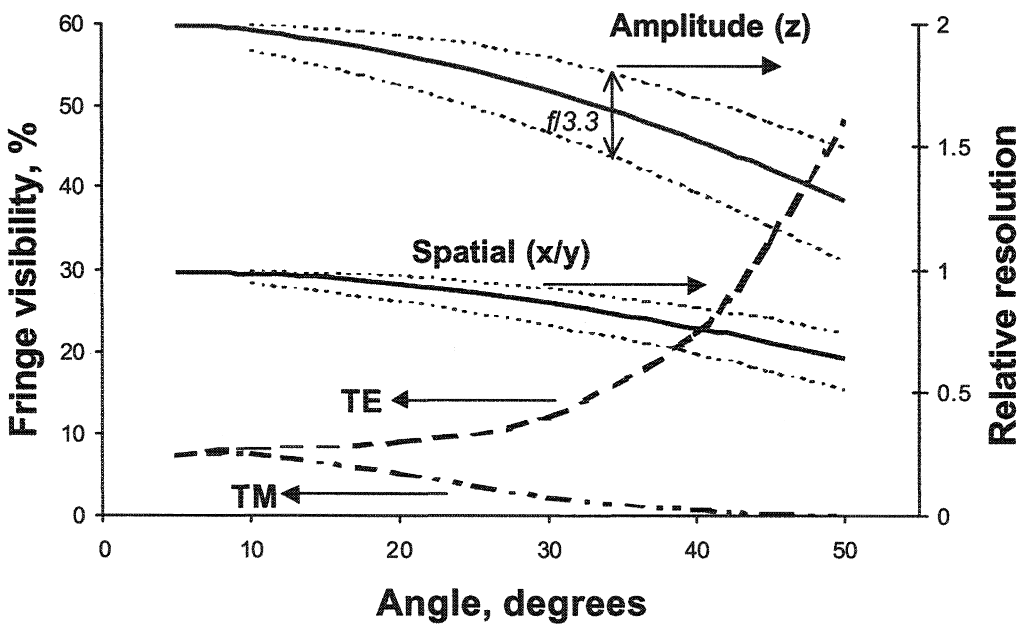

Figure 8 Calculated effect on fringe visibility and relative resolution of the angle at which the photomask is tilted with respect to the optical axis of the interferometer

For an interferometer with circularly polarization in the test cavity, (or where low tilt angles are used for TE) fringe visibility could be improved dramatically by adding a not very efficient anti-reflection coating to the reference surface of the transmission sphere; this, however, would exacerbate problems when trying to make the calibration measurements on the highly reflective sphere.

EXPERIMENTAL RESULTS

Preliminary experimental measurements were performed on a photomask substrate nominally 152 mm square by 6.25 mm thick using the NIST owned Wyko 6000 interferometer[16]. To shorten the test cavity, a 100 mm aperture f/3.3 transmission sphere was used. The return sphere has an 1125 mm nominal radius of curvature The light in the test cavity with this particular interferometer is approximately TE linearly polarized. To demonstrate the effect of polarization, a high quality uncoated 150 mm diameter fused silica flat was inserted into the test set-up (Measurement 2, Figure 2) at 45 degrees and a half-wave plate was inserted close to the focus of the transmission sphere. Rotating the half wave plate rotates the polarization, changing the fringe visibility (Figure 9). No measurements were taken of the bare test cavity (Measurement 1, Figure 2).

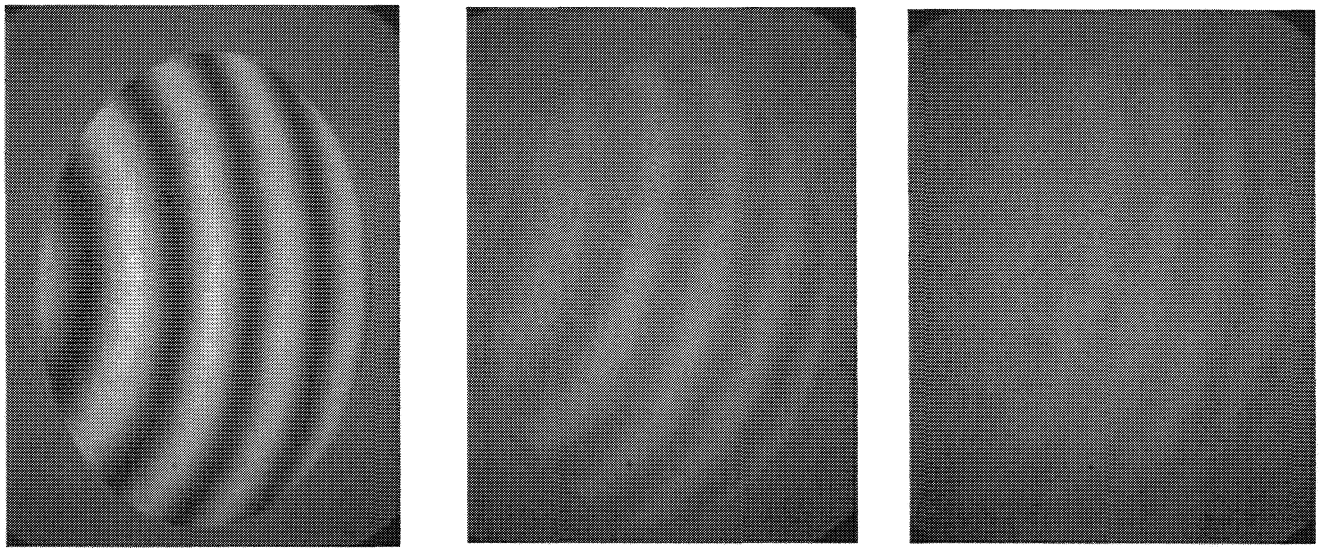

Figure 9 Raw intensity data for nominally TE (left), rotated 45 degrees (center), and nominally TM (right)

The photomask was next inserted into the test cavity and tilted approximately 45 degrees to the optical axis of the interferometer, with nominally TE incident illumination. Data was taken in this original orientation as well as with the photomask substrate rotated 90 degrees about the normal to its surface. A typical surface map as acquired by the PMI is shown in Figure 10. Figure 11 shows the processed data, remapped and optimized as indicated above. For comparison, the map in Figure 11 for the data taken with the photomask rotated a nominal 90 degrees has been rotated back such that the data are orientated in the same part coordinate system. Note the agreement both between the amplitude parameters (PV and rms) computed from the surface maps and between the reported surface shapes.

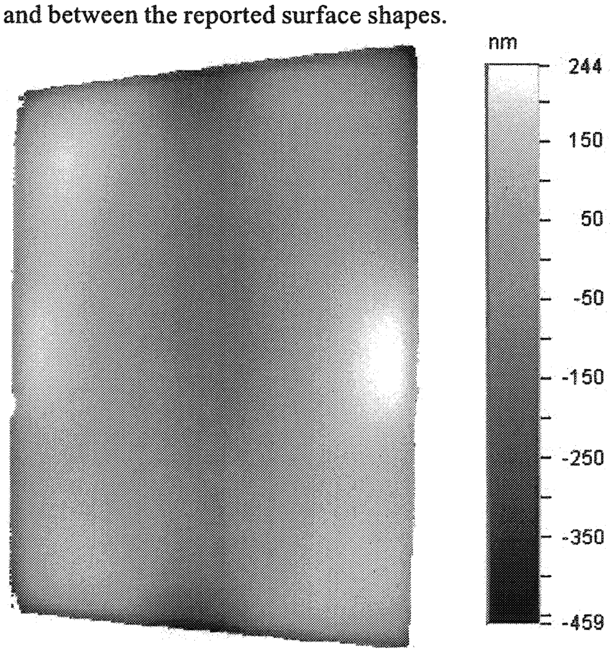

Figure 10. Raw data at nominal 0 degrees

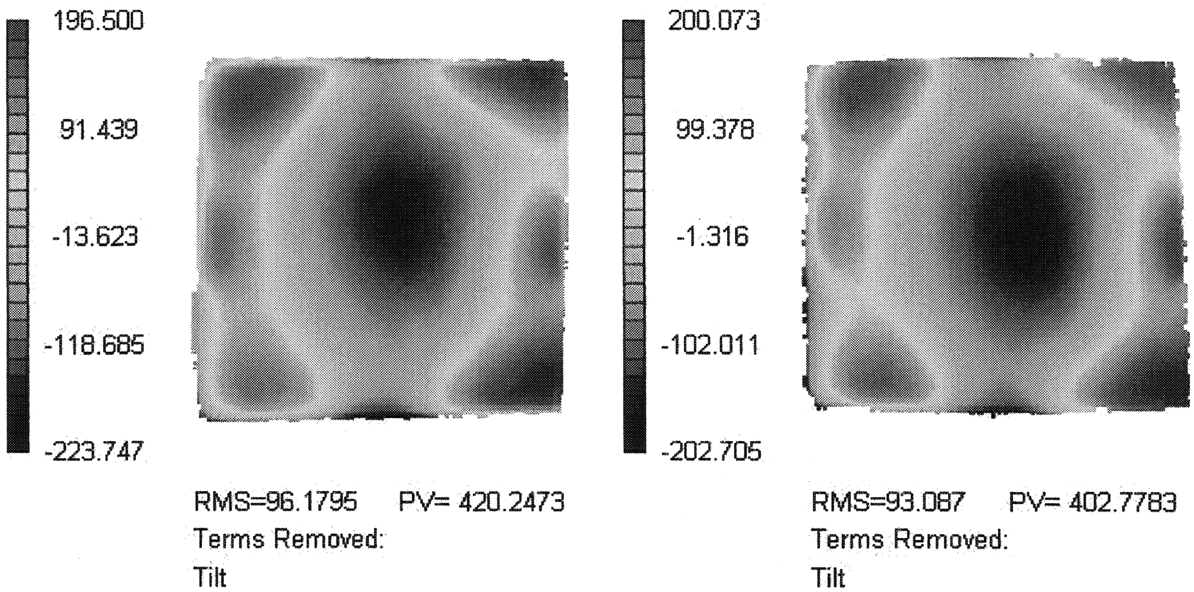

Figure 11 Processed data for nominal 0 degrees (left) and 90 degrees (right). Units are nm.

It is apparent from Figure 11 that the coordinate remapping is imperfect, presumably because the assumed tilt angle is incorrect. At 45 degrees (nominal) an error of 1 degree will result in a bias in the measurement sensitivity of approximately 2%, or approximately 2 nm rms. This uncertainty would be reduced through the use of improved tooling to align the part. Note also that if the surface figure is to be reported in terms of spatial parameters (e.g. power spectral density), then the effect of remapping error on lateral coordinates must be considered very carefully.

Other major sources of uncertainty in the preliminary data reported here are measurement noise and the departures from sphericity of the return sphere and reference surface of the transmission sphere. An assessment of the measurement noise (vibration, thermal drift, air index variation, etc) was obtained by performing 10 independent measurements and then taking the rms of the difference between arbitrary pairs of measurements. The maximum difference observed was 4 nm rms, which can be reduced by further averaging. Independent measurements indicate that the departure of the return sphere and reference surfaces from a best fit sphere are 10 nm and 4 nm rms respectively. The bias added because of non-null data is estimated as 2 nm rms. Therefore the expanded uncertainty (assuming a coverage factor, k, equal to 2) for the preliminary measurements reported in Figure 11 is 23 nm.

CONCLUDING REMARKS

This paper has shown that it is possible to make high resolution measurements of uncoated photomask substrates (and other thin, parallel windows) using the Ritchey-Common test with the types of commercially available phase shifting interferometer that is widely used in the optics industry; fringe visibility (and hence signal to noise) is dramatically improved through the use of TE linearly polarized light. The dominant contribution to the uncertainty in the results reported here is imperfections in the interferometer optics, which were not compensated. There is, however, a broad range of published approaches to reducing this bias. These preliminary results suggest that, with appropriate tooling and procedures, measurements of photomask substrates to the uncertainties needed for reflective EUVL mask are possible with existing equipment.

ACKNOWLEDGEMENTS

The authors would like to thank Peter de Groot (Zygo), Tyler Estler (NIST) and Kenneth Blaedel (Lawrence Livermore National Laboratory) for helpful comments. This work was supported by the NIST Office of Microelectronic Programs

REFERENCES

[1] Abramson N. "The Interferoscope: a new type of interferometer with variable fringe separation", Optik (Stuttgart) 30, 56-71 (1969)

[2] http://www.tropel.com/html/spec_fm200.htm

[3] "Specification for Extreme Ultraviolet Lithography Mask Substrates" SEMI Draft Document 3148, 1/16/01

[4] Blaedel K. Personal communications with CE, October 2000, February 2001

[5] Mantravadi M. V. "Newton, Fizeau and Haidinger interferometers", in Optical Shop Testing, 2nd Ed (ed D. Malacara) Wiley, 1992

[6] Evans C. J.,. Parks R. E, Shao L-Z., and Davies A. "Interferometric metrology of photomask blanks: Approaches using 633 nm wavelength illumination", NISTIR 6701, December 2000

[7] http://www.phase-shift.com/optiflat.shtml

[8] Schwider J. "White light interferometer", Applied Optics, 36(7) 1433-7 (1997)

[9] de Groot P. "Measurement of transparent plates with wavelength-tuned phase-shifting interferometry", Applied Optics, 39(16) pp2658-63 (2000)

[10] de Groot P, Deck L., and Colonna de Lega C. "Adjustable coherence depth in a geometrically desensitized interferometer", SPIE 1998 Annual Meeting Paper # 3479-02

[11] Ai C. "Multimode laser Fizeau interferometer for measuring the surface of a thin transparent plate" Applied Optics, 36(31) 8135-8 (1997)

[12] Ritchey G. W "On the Modern Reflecting Telescope and the Making and Testing of Optical Mirrors" Smithson. Contrib. Knowl., Vol 34, No 3, (1904) as quoted by Ojeda-Castenada J. in "Focault, Wire and Phase Modulation Techniques", Chapter 9 of Optical Shop Testing 1st Ed, (ed D. Malacara), Wiley, 1978.

[13] Shu K. L. "Ray-trace Analysis and Data Reduction Methods for the Ritchey-Common Test", Applied Optics, Vol 22 (12), pp1879-86, (1983)

[14] Parks R. E., Evans C. J. and Shao L-Z. "Implementation of the Ritchey-Common test for 300 mm wafers" , OSA 1998 Technical Digest Series, No 12 "Optical Fabrication and Testing" pp104-7

[15] Parks R. E., Shao L-Z., and Evans C. "Absolute Ritchey-Common test for circular flats", OSA 1996 Technical Digest Series, No 7 "Optical Fabrication and Testing" 24-7

[16] Commercially available products are identified to provide a complete description of the work. Such identification does not imply endorsement by the National Institute of Standards and technology, nor that they are necessarily best suited for the application

[17] Bruning J. H. "Fringe Scanning Interferometers" in 'Optical Shop Testing', 1st Ed, (D. Malacara, ed), pp409-437, Wiley, 1978

[18] WYKO 6000[16]